Principal bifurcations and symmetries in the emergence of reaction-diffusion-advection patterns on finite domains

Arik Yochelis* and Moshe Sheintuch†

Department of Chemical Engineering, Technion-Israel Institute of Technology, Haifa 32000, Israel

(Received 27 October 2008; revised manuscript received 12 July 2009; published 2 November 2009)

Pattern formation mechanisms of a reaction-diffusion-advection system, with one diffusivity, differential advection, and (Robin) boundary conditions of Danckwerts type, are being studied. Pattern selection requires mapping the domains of coexistence and stability of propagating or stationary nonuniform solutions, which for the general case of far from instability onsets, is conducted using spatial dynamics and numerical continuations. The selection is determined by the boundary conditions which either preserve or destroy the translational symmetry of the model. Accordingly, we explain the criterion and the properties of stationary periodic states if the system is bounded and show that propagation of nonlinear waves (including solitary) against the advective flow corresponds to coexisting family that emerges nonlinearly from a distinct oscillatory Hopf instability. Consequently, the resulting pattern selection is qualitatively different from the symmetric finite wavenumber Turing or Hopf instabilities.

I. INTRODUCTION

The display of spatiotemporal self-organization by out of equilibrium systems is both rich and profound [1]. Reaction-diffusion (RD) systems constitute a major part in the study of self-organization [2–4]; theoretical and experimental studies in this framework showed many similarities between such seemingly different media such as chemical liquid-phase reactions and developmental biology systems [5,6]. While traditionally analysis (linear or weakly nonlinear) near critical point is implemented [7,8], many behaviors far from any onset cannot be captured via the center manifold framework, including pattern selection mechanisms, the respective basins of attraction, and the effect of boundary conditions (BCs) [1,9]. To this end, coupling between *spatial dynamics* and *numerical continuation* methods has proven efficient to investigate nonlinear behavior in RD type systems (for example, see [10–18]), and in particular successful in advancing the mechanisms behind localized states that are reversible in space [19].

Open flow systems, where the transport is controlled by both diffusion and a *symmetry-breaking* (differential) advection, and thus often referred to as reaction-diffusion-advection (RDA) systems [20], have attracted less attention in spite of their significance in technological and biological systems. Particularly, under certain conditions the flow may increase the stability of a system since weak perturbations are advected and on finite domains disappear from the system [21]. Although RDA systems impose a spatial symmetry breaking, they display a large plethora of qualitatively similar spatiotemporal phenomena in a wide range of contexts [22–36], including traveling waves (TW) and stationary periodic (SP) states. Theoretical understanding of the effect of nonlinear instabilities and BCs on pattern selection in RDA

systems was attempted through a weakly nonlinear analysis [26,29,37–40]; however, a framework that reveals the mechanistic understanding of the far from instability onsets behaviors is still missing.

Here we suggest a generalized methodology for the primary nonlinear (far from any instability point) properties and pattern selection mechanisms of *periodic* and *localized* states in an RDA system. As we show in Sec. II, our methods are based on linear analysis on unbounded domains followed by a numerical continuation of nonlinear solutions on periodic domains; the results both predict (amplitude and wavelength) and agree with direct numerical computations of a model equation with realistic BCs. Through a minimal model, we show that the key to nonlinear pattern selection lies in unfolding the coexistence regions of nonuniform solutions. The latter can be available using ideas from spatial dynamics [10–18], i.e., looking at steady states in a comoving reference. Furthermore, we explain using translational symmetry considerations of spatial solutions that BCs in a laboratory reference act as a selection mechanism (effective stabilization) to form either propagating or stationary states.

This type of analysis allows us also understanding of the onset of upstream propagating (against the advective direction) waves and the accompanied excitable pulses regions, as described in Sec. IV; the latter are beyond the scope of weakly nonlinear analysis [1,29]. The insights in principle, appear as model independent and thus their validity to a broad class of simple RDA models is anticipated [22–36]; examples may include chemical reactions subjected to an electric field [41], membrane reactors [42], axial segmentation in vertebrates [43,44], biochemical oscillations in an amoeboid organism Physarum [45], autocatalytic reactions on a rotating disk [46], and vegetation patterns [47]. In Sec. V, we discuss the generality of the results in more detail.

II. MODEL EQUATIONS AND LOCAL BIFURCATIONS

We begin, without a loss of generality, with an RDA model of a membrane (or cross-flow) reactor, which in dimensionless form reads [42]

*Present address: Landa Labs, P.O. Box 4060, Nes Ziona 74140, Israel. arik.yochelis@landalabs.com

†cermsll@technion.ac.il

$$\frac{\partial u}{\partial t} + \frac{\partial u}{\partial x} = f(u,v) - u,$$

$$\text{Le}\frac{\partial v}{\partial t} + \frac{\partial v}{\partial x} = Bf(u,v) - \alpha v + \frac{1}{\text{Pe}}\frac{\partial^2 v}{\partial x^2}. \qquad (1a)$$

The equations represent a tubular reactor with continuous feeding and cooling in which an exothermic (Arrhenius kinetics) reaction takes place

$$f(u,v) = \text{Da}(1 - u)e^{\gamma v/(\gamma + v)}. \qquad (1b)$$

In Eq. (1), $u(x,t)$ and $v(x,t)$ stand for conversion and temperature, respectively; $u=1$ implies zero reactant concentration.

Unless stated otherwise, the BCs that are used in all direct numerical computations are Robin

$$a_u u + b_u \frac{\partial u}{\partial x} = g_u, \quad a_v v + b_v \frac{\partial v}{\partial x} = g_v \quad \text{at } x = 0, \quad (2a)$$

and no-flux

$$\frac{\partial v}{\partial x} = 0 \quad \text{at } x = L, \qquad (2b)$$

where L is the physical domain size, and $a_{u,v}$, $b_{u,v}$, and $g_{u,v}$ are real constants. We use a specific form of Danckwerts type [42], that is at the inlet ($x=0$)

$$(a_u, b_u, g_u) = (1, 0, 0), \qquad (2c)$$

and

$$(a_v, b_v, g_v) = (1, -1/\text{Pe}, 0). \qquad (2d)$$

However, qualitatively similar results are obtained with other BCs, for example Dirichlet BCs.

In the absence of spatial derivatives, Eq. (1) admits distinct uniform steady states [48],

$$\begin{pmatrix} u \\ v \end{pmatrix} = \begin{pmatrix} u_0 \\ v_0 \equiv Bu_0/\alpha \end{pmatrix}, \qquad (3)$$

as solutions of

$$\text{Da} = \frac{u_0}{1 - u_0} e^{-\gamma u_0/(\gamma \alpha/B + u_0)}.$$

In what follows, we set the Lewis number, Le$=100$, while other parameters $B=16.2$, $\alpha=4$, $\gamma=10\,000$ (see [42] for details), and use the Damköhler number, Da, and the Péclet number, Pe, as control parameters allowed to vary. Le is the ratio of solid- to fluid-phase heat capacities, Pe is the ratio of convective to conductive enthalpy fluxes, Da is the dimensionless rate constant, and B stands for exothermocity. The parameter choices and the BCs are considered as realistic [42].

Since Eq. (1) contains only one diffusive term, the Turing mechanism that is known to operate in RD systems with two diffusing subsets is excluded [1,49]. Nevertheless, numerical integrations of Eq. (1), with Danckwerts BCs, showed that above a critical Pe value, an asymptotic SP pattern emerges via an instability of the uniform state to TW [29]. An under-

standing of such behavior has been attempted by looking at a weakly nonlinear reduction around a special point, referred to as an "amplification threshold." However, the phenomenon remains unclear since a formal center manifold cannot be identified.

In the following, we show that a combination between linear (assuming infinite domains) analysis of Eq. (1) and of a reduced system in a comoving frame (on periodic domains) provides the desired information about the origin of both TW and SP states. Finally, we demonstrate that the role of BCs on large domains is to select among the two types of solutions, although mixed Robin BCs formally exclude the existence of spatially uniform states.

A. Linear theory

To analyze the primary instability of nonuniform states and the effect of advection/diffusion we assume first an infinite domain, i.e., neglecting BCs; we vary Pe while keeping Da$=0.2$ for which $(u_0, v_0) \simeq (0.872, 3.533)$. A standard linear stability analysis to infinitesimal periodic perturbations [1]

$$\begin{pmatrix} u \\ v \end{pmatrix} = \begin{pmatrix} u_0 \\ v_0 \end{pmatrix} + \epsilon \begin{pmatrix} u_k \\ v_k \end{pmatrix} e^{\sigma t + ikx} + \text{c.c.} + \mathcal{O}(\epsilon^2), \qquad (4)$$

yields two complex dispersion relations, $\sigma = \sigma_{\pm}(k)$, where σ is the (complex) perturbation growth rate, $k>0$ is the wavenumber, and $\epsilon \ll 1$. The two are computed numerically while only $\sigma_+(k)$ exhibits an oscillatory finite wavenumber Hopf bifurcation at Pe$=$Pe$_W$, i.e., Re$[\sigma_+(k=k_W \simeq 6.68)]=0$ and Re$[\sigma_+(k)]<0$ otherwise, for details see the top inset in Fig. 1(a).

The advective terms in Eq. (1) break the reflection symmetry of the finite wavenumber Hopf bifurcation, and the emergence of counter propagating waves and standing waves [50]. Instead only one type of waves is selected, corresponding to the frequency $\omega(k) = \omega_W \equiv \text{Im}[\sigma_+(k_W)] \simeq -0.0006$ at the onset. Under the above choice of parameters and beyond Pe$_W$, the uniform state (on an infinite domain) is convectively unstable to TW [21].

B. Spatial bifurcation to traveling wave

As we showed above, the primary bifurcation is to TW; thus the origin of the forming SP states under aperiodic BCs [Fig. 1(b)] is hidden. To unfold the behavior of both TW and SP, we need to show first existence, and thus consider Eq. (1) in a comoving frame, $\xi = x - ct$,

$$\frac{du}{d\xi} = \frac{f(u,v) - u}{1 - c},$$

$$\frac{dv}{d\xi} = w,$$

$$\frac{dw}{d\xi} = \text{Pe}[(1 - c\text{Le})w - Bf(u,v) + \alpha v]. \qquad (5)$$

The negative sign before c was set since at the onset, Im$[\sigma_+(k_W)]<0$. Thus, solutions with $c>0$ ($c<0$) corre-
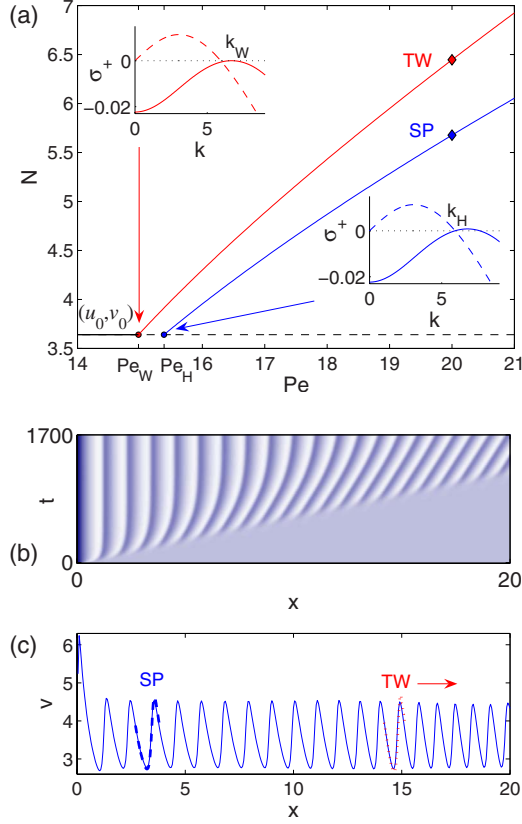
FIG. 1. (Color online) (a) Bifurcation diagram for spatially homogeneous (u_0, v_0) steady states [solid (stable) and dashed (unstable) dark lines] and distinct spatially periodic (light lines) solutions. All the solutions were computed using Eq. (5) at Da=0.2, and represented in terms of N [see Eq. (7)], as a function of Pe. Traveling waves (TW) emerge from a finite wavenumber Hopf bifurcation at Pe=Pe$_W \simeq 14.976$ and $\lambda_W \equiv 2\pi/k_W \simeq 0.94$. Stationary periodic (SP) solutions emerge from Pe=Pe$_H \simeq 15.387$, for which Re$[\sigma_+(k_H)]$=Im$[\sigma_+(k_H)]$=0. The branches of nonuniform states were computed on periodic domains, $L=\lambda_W$ for TW and for SP $L=\lambda$ is varied with Pe. The insets represent the real (solid line) and the imaginary (dashed line) parts of the respective dispersion relations at Pe=Pe$_W$ and Pe=Pe$_H$. (b) Space-time plot where dark color indicates larger v field values; Eq. (1) was integrated starting from $[u(x,t=0), v(x,t=0)]=[u_0, v_0]$, at Pe=20 with Danckwerts boundary conditions [see Eq. (2)]. (c) A Spatial profile of $v(x)$ at t=1700. The dashed (dotted) line indicates the corresponding single period profile of SP (TW) state, obtained via the continuation method [diamond symbols in (a)].

spond to downstream (upstream) propagating waves.

The existence and the properties of nonuniform states can be now approached via a spatial dynamics analysis [10–18]. Linearization about the uniform state results in solutions which admit

$$\begin{pmatrix} u \\ v \\ w \end{pmatrix} - \begin{pmatrix} u_0 \\ v_0 \\ 0 \end{pmatrix} \propto e^{\mu \xi}, \qquad (6)$$

where the spatial eigenvalues μ satisfy a third-order algebraic equation. At Pe=Pe$_W$ and $c=c_W \equiv |\omega_W|/k_W \simeq 0.0009$,

the three spatial eigenvalues are: $\mu_\pm = \pm i k_W$ and $\mu > 0 \in \mathbb{R}$. For Pe$\lesssim$Pe$_W$, $\mu_\pm \in \mathbb{C}$ with Re$(\mu_\pm)<0$, corresponding to a saddle focus [51–53], while for Pe$\gtrsim$Pe$_W$, $\mu_\pm \in \mathbb{C}$ with Re$(\mu_\pm)>0$ corresponding to periodic orbits, i.e., TW in context of Eq. (1).

The branch of TW bifurcates supercritically from Pe=Pe$_W$ and computed on periodic domains using the numerical continuation package AUTO [54], by two parameter variation (Pe,c) while the period $\lambda = \lambda_W \equiv 2\pi/k_W$ remains fixed, as shown in Fig. 1(a). The results are presented in terms of a norm that accounts both the field values and the derivatives to better distinguish between distinct nonuniform solutions [54]

$$N = \sqrt{\frac{1}{\lambda} \int_0^\lambda \left[u^2 + v^2 + w^2 + \left(\frac{du}{d\xi}\right)^2 + \left(\frac{dv}{d\xi}\right)^2 + \left(\frac{dw}{d\xi}\right)^2 \right] d\xi}.$$
(7)

Consequently, the domain period λ becomes an effective control parameter, implying the coexistence of other nonuniform states that are also solutions to Eq. (5).

C. Spatial bifurcation to stationary periodic states

While the onset for SP solutions is absent via Eq. (4), one can study their onset in the context of Eq. (5). These states bifurcate in the same (supercritical) direction but from Pe=Pe$_H \simeq 15.387$, which is exactly the so-called "amplification threshold" discussed in [29], corresponding to Re$[\sigma(k_H)]$=Im$[\sigma(k_H)]$=0 [see bottom inset in Fig. 1(a)]. In this case, we employed variation in parameters (Pe,λ) while the speed was fixed to $c=0$, which is identical to SP states in the context of Eq. (1). Note that in general TW at Pe=Pe$_H$ can exceed the validity of small amplitude states.

III. BOUNDARY CONDITIONS AND SELECTION BY SYMMETRY

Both the TW and the SP solutions discussed above arise in supercritical bifurcations and thus expected to enslave the spatiotemporal evolution that emerges from perturbations around the uniform state (u_0, v_0). Here we show that this is indeed in a good agreement with integration of Eq. (1), on relatively large domains, i.e., $L \gg \lambda$.

Temporal stability computations show that TW are stable to long-wavelength perturbations. The stability was computed for large periodic domains, $L=n\lambda_W$, with integer n > 1 (until the onset didn't change with n), via a standard numerical eigenvalue method using Eq. (1), in a comoving frame. Thus, with periodic BCs, $x \to x+n\lambda$, that preserve the translational symmetry of Eq. (1), the bifurcating downstream TW are readily stable while due to the convective instability with purely no-flux BCs at the inlet (although non-physical), TW are swept from the domain leaving a uniform state behind [28].

On the other hand, on finite domains (not necessarily $L=n\lambda$) with a forced boundary that breaks the translational symmetry, such as Danckwerts BCs, TW are transient: after they emerge, they propagate toward the right boundary and

disappear [see Fig. 1(b)]. Instead these conditions select the SP states which are unstable on periodic domains. We note that since here standing-wave patterns are excluded (due to the presence of differential advection), also spatially localized oscillations should not form, leading the SP patterns (with possible defects) to be the only attractor of the system. As such, formation of SP patterns does not require two diffusing fields (a Turing type mechanism) [55].

This mechanism is also supported by the profiles comparison of TW and of SP states obtained via direct integration of Eq. (1) and by a continuation method, as represented in Fig. 1(c). Thus, solutions' properties of (1) are indeed result from spatial instabilities in the comoving frame (5), and the BCs act as a selection mechanism. Importantly, below $Pe=Pe_H$, SP cannot form and the solutions indeed show a spatially oscillating decay from $x=0$ to the (u_0,v_0) at $x=L$ due to the complex eigenvalues with negative real parts.

IV. NONLINEAR BIFURCATIONS AND UPSTREAM PROPAGATION

In the previous sections, we showed that the spatiotemporal evolution is enslaved to downstream propagating TW due to the supercritical property of the primary Hopf bifurcation. However, Hopf bifurcation can be also of a subcritical (nonlinear) type, and as we will show, such an instability is responsible for the formation of upstream propagating TW. Moreover, since a subcritical finite wavenumber Hopf bifurcation is related to the emergence of solitary waves [56], we provide a mechanistic identification of excitable region also in our model.

A. Upstream propagating traveling waves

We start with a fix $Pe=Pe_W$ and vary Da. Since Da controls the uniform state (u_0,v_0) [see Fig. 2(a)], it allows formation of an additional finite wavenumber Hopf bifurcation: the top and the bottom uniform states go through a finite wavenumber Hopf bifurcation at $Da=Da_W^\pm$, and we refer to the periodic bifurcating states as TW$^+$ and TW$^-$, respectively.

Unlike in the supercritical case (Da_W^+ onset), the onset of TW$^-$, admits $Im[\sigma_+(k)]<0$, for $k>0$ and $Im[\sigma_+(k=0)]=0$. Furthermore, continuation [using (5)] from the onset (with $c_W^-\simeq0.007$ at the onset), reveals that the TW$^-$ branch extends first toward small Da values, folds and extends toward large Da values and after additional fold the branch terminates at (u_0,v_0), as shown in Fig. 2(a). In the comoving frame this termination is a Hopf bifurcation, however there is no bifurcation analog in the context of Eq. (1). The two limiting subcritical bifurcations, imply that the solutions along the middle part of the branch are of large amplitude. Importantly, the speed of TW$^-$ changes sign after the left saddle node, $Da\simeq0$, and thus, the branch that extends to large Da values corresponds to upstream propagating TW with a period $\lambda_W^-\simeq3.06\sim3\lambda_W^+$ [see inset in Fig. 2(a)].

Again, direct numerical integration of Eq. (1) agrees with the latter: a boundary perturbation (which is 'large') advected first with the flow (downstream), but giving rise to upstream propagating waves [see Figs. 2(b) and 2(c)].
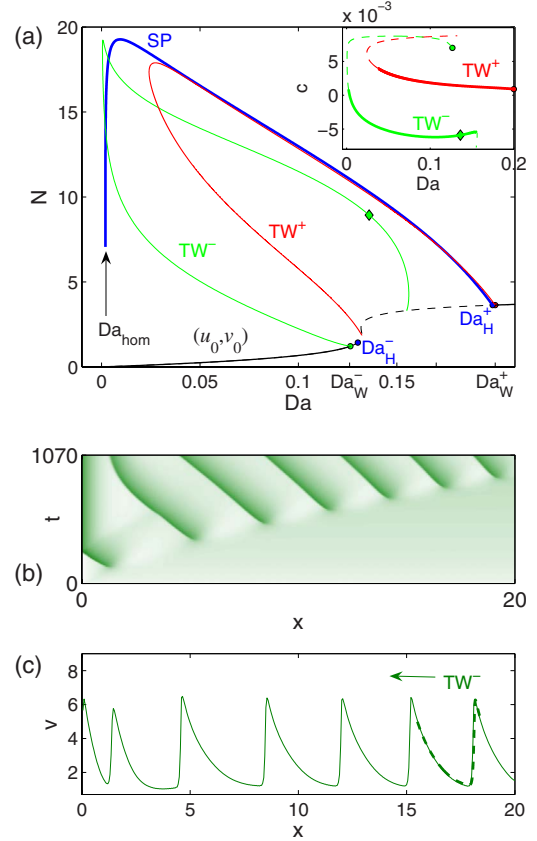
FIG. 2. (Color online) (a) Bifurcation diagram for coexisting uniform (dark lines) and nonuniform (light lines) solutions, as a function of Da at $Pe\simeq14.976$. The two types of traveling waves, TW$^\pm$, bifurcate respectively from $Da=Da_W^+=0.2$ and $Da_W^-\simeq0.1264$; the TW$^-$ have a longer period $\lambda_W^-\simeq3.06$, as compared to the TW$^+$ [$\lambda_W^+\equiv\lambda_W$ in Fig. 1(a)]. The thick line represents SP states that bifurcate from $Da=Da_H^+\simeq0.1987$ and approach a homoclinic orbit at $Da_{hom}\simeq0.002$ (a pulse state with $L=\lambda\to\infty$). $Da=Da_H^-\simeq0.1302$ marks the second onset of stationary periodic states. The branches of nonuniform states of Eq. (5) were computed numerically on periodic domains, $L=\lambda_W^+$ for TW$^+$, $L=\lambda_W^-$ for TW$^-$, and for SP $L=\lambda$ is varied (increased) as Da is decreased (see Fig. 3). The inset shows the stable parts (thick line) of TW$^\pm$ branches in terms of c (see text for details). (b) Space-time plot where dark color indicates larger values of the $v(x,t)$ field; integration of Eq. (1) as in Fig. 1(b) at $Da=0.136$ and $Pe=Pe_W$. (c) Profile of $v(x)$ at $t=1070$ [see (b)]; dashed line indicates the corresponding single period profile of TW$^-$ [diamond symbol in (a)].

Namely, above threshold perturbations will converge to the coexisting large amplitude TW$^-$. As in the previous section, due to the use of Danckwerts BCs these upstream propagating waves are transient. Thus, formation of upstream waves (TW$^-$) cannot be attributed to a secondary instabilities of the primary TW$^+$ but rather to branch switching via a large amplitude (nonlinear) perturbation and as such could not be anticipated nor understood via a weakly nonlinear analysis around $Da=Da_W^+$ [29,39].

B. Excitability and solitary waves

Finally, we turn to an identification of spatially localized states and solitary waves which as we show are intimately
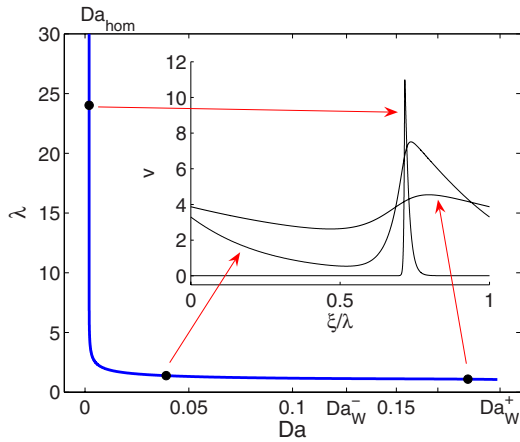
FIG. 3. (Color online) A branch of stationary nonuniform solutions ($c=0$ along the branch), i.e., the SP branch from Fig. 2(a), portrayed in terms of domain size, $L=\lambda$. The inset shows profiles of $v(\xi)$ normalized by the domain period. Integration details and parameters as in Fig. 2(a).

connected to the bifurcating SP states and can be anticipated due to a subcritical nature of the upstream waves (TW$^-$), for more details see [56].

As in the first studied case, Pe variation, SP states also bifurcate (in the same directions as the TW$^\pm$) in respective vicinities of Da$=$Da$_W^\pm$. In Fig. 2(a) we mark the two onsets as Da$=$Da$_H^\pm$ but present for simplicity only the branch that bifurcates from Da$=$Da$_H^+$. Computation of SP states results in termination of the latter on a homoclinic orbit (a pulse state where $\lambda \to \infty$), at Da$\equiv$Da$_{hom} \simeq 0.002$ [see thick (blue) line in Fig. 2(a) and Fig. 3]. Termination at low Da values can be also supported by the spatial eigenvalues configuration for Da$\lesssim$Da$_W^-$, i.e., the onset of a saddle focus [51–53]. Thus, also other homoclinic orbits can be present, these correspond to propagating solitary waves ($c \neq 0$) or excitable pulses [see Fig. 4(a)].

To capture these spatially localized solutions, we implement a homotopy method [54]: we initialize the continuation scheme on a stationary localized state at Da$=$Da$_{hom}$ which was obtained following the SP branch, fix a relatively large period, and vary simultaneously Da and c. Figure 4(a) shows the branches of upstream ($c<0$) and downstream ($c>0$) propagating pulses. We find that the low amplitude pulses ($c>0$) are unstable while the large amplitude pulses ($c<0$) are stable. Above Da$_W^-$, solitary waves cannot stabilize due to a linear instability of the uniform state [see Fig. 2(a)]. The resulting branches do not change by a period increase.

To access the basin of attraction of the transient pulse we induced a finite amplitude symmetric top-hat perturbation at Da$=0.1<$Da$_W^-$, which initially propagates downstream as a small amplitude pulse and by reaching a critical amplitude, changes the propagation direction, as shown in Fig. 4(b); the large amplitude profile is not dependent on the location of the stimuli or extension of the domain size. Figure 4(c) shows that the profile of a propagating pulse under Danckwerts BCs (solid line) agrees with the profile obtained using Eq. (5) on a periodic domain. Note that since $v(\xi)$ was computed on a larger domain ($L=24$), only part of it is plotted. In addition, we emphasize that the profile discrepancy near the
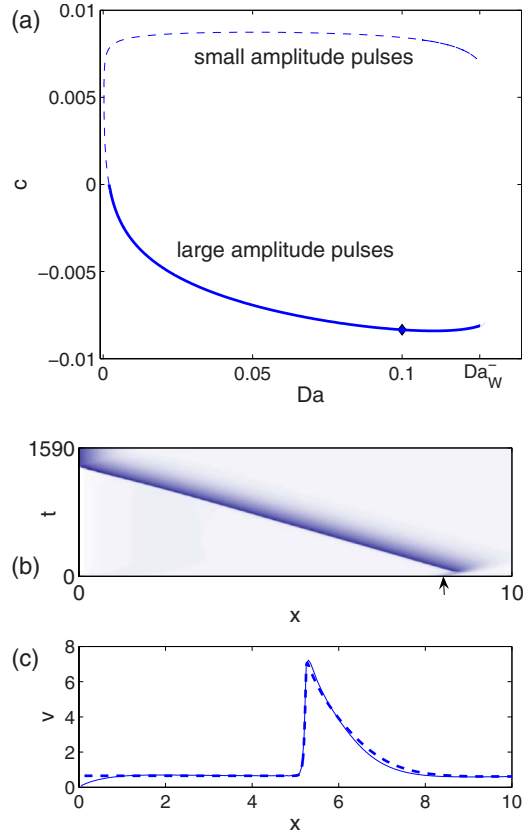
FIG. 4. (Color online) (a) Branches of a single pulse state computed using Eq. (5) on a large domain, with variation in (Da,c) while other parameters as in Fig. 2(a); solid (dashed) lines mark stable (unstable) solutions on the whole line. The periodic domain used for such computations is $L=\lambda=24$, noting that the results do not change once the domain size is increased. (b) Space-time plot where dark color indicates larger values of the $v(x,t)$ field, showing the formation and the propagation a solitary wave from a single spatially localized perturbation (the location is marked by an arrow); integration of Eq. (1) as in Fig. 1(b) at Da$=0.1$ and Pe$=$Pe$_W$. (c) Profile of $v(x)$ at an intermediate time, where the dashed line indicates the corresponding profile of a pulse $v(\xi)$, obtained by continuation [diamond symbol in (a)].

inlet ($x=0$), does not modify the excitable region in the far field, that is far from the left boundary. Asymptotically the pulse propagates toward the left boundary and arrests there, so that in principle a finite period train can be generated near the inlet by repetitive perturbations. The periodicity of such bounded stationary states, corresponds to periodicity of the coexisting SP states at the respective Da value [see Fig. 2(a)].

We note that upstream propagating excitable pulses have been observed experimentally using distinct Belousov-Zhabotinsky based chemical preparations [41,57,58]. Using numerical simulations of FitzHugh-Nagumo model, it was conjectured that the phenomenon underlines identical flow and diffusion coefficients [58]. However, as we mechanistically showed a model with two diffusing fields is not a prerequisite for excitable behavior in RDA media.

V. CONCLUSIONS

In this study, we showed that the fundamental spatiotemporal behavior in RDA systems with mixed Robin BCs, can be efficiently deduced by properties of spatially periodic and localized solutions that are present in a comoving coordinate system on periodic domains, i.e., employing ideas from spatial dynamics and the use of a numerical continuation such as the AUTO package [54]. These methods extend the results obtained via weakly nonlinear analysis [29,37–40], and thus, allowed us a mechanistic exploration in the fully nonlinear regime. Moreover, we showed that the basic bifurcations are already present in a nonlinear RDA model with only one diffusive field. The latter provides a distinct rationale since in the absence of a differential advection, finite wavenumber bifurcations (stationary or oscillatory) cannot occur. The main results can be summarized as following:

(i) Under certain conditions, BCs that break the symmetry of TW [here of Danckwerts type, i.e., Eq. (2)], mainly act to select SP states: once the translational symmetry of Eq. (1) is broken (by the BCs), SP states may asymptotically stabilize, providing the existence of a Hopf bifurcation in a comoving reference frame with $c=0$ (see Sec. III).

(ii) The presence of a subcritical finite wavenumber Hopf bifurcation gives rise to upstream propagating periodic and solitary waves (see Sec. IV). Such details allowed us to explain the speed reversal of TW which is associated with subcriticality (nonlinear instability) of one of the Hopf bifurcations and thus to a distinct family of waves. The solitary waves are asymmetric homoclinic orbits in space, and act as generic organizing centers of (nonuniform) spatial solutions [51–53].

(iii) The mechanism behind SP states does not stem from a Turing type instability: in systems such as (1) there is a single diffusion term, and thus the onset of SP patterns in system (5) is not of a reversible Hopf (i.e., preserving $x \rightarrow -x$ symmetry) type as in the Turing case [49]. In addition, properties of solitary waves which are irreversible homoclinic orbits in space, are generic solutions of a three component ODE, which results from a two component PDE with a single diffusion. Consequently, these results imply that the mechanisms behind generic formation of SP states and excitable pulses, do not require two diffusing fields.

All the above, present both rich and complex mechanisms that shape the formation of RDA patterns. Naturally, many further questions arise about the secondary bifurcations, sensitivity to initial conditions vs the domain size. However these are beyond the scope of this paper and addressed in a companion paper [59].

We find the generation of solitary waves and finite periodic trains near the inlet in a cross-flow reactor (an analog to hot spot arrays), to be of high technological importance. Moreover, due to the organization around nonlinear bifurcations, the results appear as model independent and indeed were numerically found in diversity of simple RDA models [22–36]. Thus, we hope that the insights provided here will trigger further technological explorations of physicochemical systems [20,41,42,46,57,58,60], and inspire ideas to biological [43–45,61–63] and ecological [47], applications.

[1] M. C. Cross and P. C. Hohenberg, Rev. Mod. Phys. **65**, 851 (1993).

[2] R. Kapral and K. Showalter, *Chemical Waves and Patterns* (Kluwer, Dordrecht, 1995).

[3] P. K. Maini, K. J. Painter, and H. N. P. Chau, J. Chem. Soc., Faraday Trans. **93**, 3601 (1997).

[4] I. R. Epstein and J. A. Pojman, *An Introduction to Nonlinear Chemical Dynamics: Oscillations, Waves, Patterns and Chaos* (Oxford University Press, New York, 1998).

[5] J. Keener and J. Sneyd, *Mathematical Physiology* (Springer-Verlag, New York, 1998).

[6] J. D. Murray, *Mathematical Biology* (Springer-Verlag, New York, 2002).

[7] L. M. Pismen, *Patterns and Interfaces in Dissipative Dynamics* (Springer-Verlag, Berlin, 2006).

[8] R. B. Hoyle, *Pattern Formation: An Introduction to Methods* (Cambridge University Press, Cambridge, 2006).

[9] E. Knobloch, in *Nonlinear Dynamics and Chaos: Where Do We Go from Here?*, edited by S. J. Hogan *et al.* (IOP, London, 2002).

[10] A. R. Champneys, Physica D **112**, 158 (1998).

[11] P. D. Woods and A. R. Champneys, Physica D **129**, 147 (1999).

[12] D. Gomila, A. J. Scroggie, and W. J. Firth, Physica D **227**, 70 (2007).

[13] J. Burke and E. Knobloch, Chaos **17**, 037102 (2007).

[14] J. Burke, A. Yochelis, and E. Knobloch, SIAM J. Appl. Dyn. Syst. **7**, 651 (2008).

[15] J. H. P. Dawes, SIAM J. Appl. Dyn. Syst. **7**, 186 (2008).

[16] A. Yochelis and A. Garfinkel, Phys. Rev. E **77**, 035204(R) (2008).

[17] D. J. B. Lloyd, B. Sandstede, D. Avitabile, and A. R. Champneys, SIAM J. Appl. Dyn. Syst. **7**, 1049 (2008).

[18] S. M. Houghton and E. Knobloch, Phys. Rev. E **80**, 026210 (2009).

[19] E. Knobloch, Nonlinearity **21**, T45 (2008), and references therein.

[20] A. B. Rovinsky and M. Menzinger, Phys. Rev. Lett. **70**, 778 (1993).

[21] P. Huerre and P. A. Monkewitz, Annu. Rev. Fluid Mech. **22**, 473 (1990).

[22] A. B. Rovinsky and M. Menzinger, Phys. Rev. Lett. **69**, 1193 (1992).

[23] S. Ponce Dawson, A. Lawniczak, and R. Kapral, J. Chem.

Phys. **100**, 5211 (1994).

[24] S. P. Kuznetsov, E. Mosekilde, G. Dewel, and P. Borckmans, J. Chem. Phys. **106**, 7609 (1997).

[25] M. Sheintuch, Physica D **102**, 125 (1997).

[26] R. A. Satnoianu, J. H. Merkin, and S. K. Scott, Physica D **124**, 345 (1998).

[27] P. Andresén, M. Bache, E. Mosekilde, G. Dewel, and P. Borckmanns, Phys. Rev. E **60**, 297 (1999).

[28] J. R. Bamforth, S. Kalliadasis, J. H. Merkin, and S. K. Scott, Phys. Chem. Chem. Phys. **2**, 4013 (2000).

[29] O. A. Nekhamkina, A. A. Nepomnyashchy, B. Y. Rubinstein, and M. Sheintuch, Phys. Rev. E **61**, 2436 (2000).

[30] R. A. Satnoianu and M. Menzinger, Phys. Rev. E **62**, 113 (2000).

[31] J. R. Bamforth, S. Kalliadasis, J. H. Merkin, and S. K. Scott, Phys. Chem. Chem. Phys. **3**, 1435 (2001).

[32] O. Nekhamkina and M. Sheintuch, Phys. Rev. E **66**, 016204 (2002).

[33] O. Nekhamkina and M. Sheintuch, Phys. Rev. E **68**, 036207 (2003).

[34] I. Kiss, J. H. Merkin, S. K. Scott, and P. L. Simon, Q. J. Mech. Appl. Math. **57**, 467 (2004).

[35] E. H. Flach, S. Schnell, and J. Norbury, Phys. Rev. E **76**, 036216 (2007).

[36] D. A. Vasquez, J. Meyer, and H. Suedhoff, Phys. Rev. E **78**, 036109 (2008).

[37] M. C. Cross, Phys. Rev. Lett. **57**, 2935 (1986).

[38] M. C. Cross and E. Y. Kuo, Physica D **59**, 90 (1992).

[39] J. M. Chomaz, Phys. Rev. Lett. **69**, 1931 (1992).

[40] S. M. Tobias, M. R. E. Proctor, and E. Knobloch, Physica D **113**, 43 (1998).

[41] H. Sevčíková, M. Marek, and S. C. Müller, Science **257**, 951 (1992).

[42] O. Nekhamkina, B. Y. Rubinstein, and M. Sheintuch, AIChE J. **46**, 1632 (2000).

[43] M. Kærn, M. Menzinger, R. Satnoianu, and A. Hunding, Faraday Discuss. **120**, 295 (2002).

[44] H. Nagahara, Y. Ma, Y. Takenaka, R. Kageyama, and K. Yoshikawa, Phys. Rev. E **80**, 021906 (2009).

[45] H. Yamada, T. Nakagaki, R. E. Baker, and P. K. Maini, J.

Math. Biol. **54**, 745 (2007).

[46] Y. Khazan and L. M. Pismen, Phys. Rev. Lett. **75**, 4318 (1995).

[47] F. Borgogno, P. D'Odorico, F. Laio, and L. Ridolfi, Rev. Geophys. **47**, RG1005 (2009).

[48] A. Uppal, W. H. Ray, and A. B. Poore, Chem. Eng. Sci. **29**, 967 (1974).

[49] A. Yochelis, Y. Tintut, L. L. Demer, and A. Garfinkel, New J. Phys. **10**, 055002 (2008).

[50] J. D. Crawford and E. Knobloch, Annu. Rev. Fluid Mech. **23**, 341 (1991).

[51] J. Guckenheimer and P. Holmes, *Nonlinear Oscillations, Dynamical Systems, and Bifurcations of Vector Fields* (Springer-Verlag, New York, 1983).

[52] Yu. A. Kuznetsov, *Elements of Applied Bifurcation Theory* (Springer-Verlag, New York, 1995).

[53] L. P. Shilnikov, A. L. Shilnikov, D. V. Turaev, and L. O. Chua, *Methods of Qualitative Theory in Nonlinear Dynamics, Part II* (World Scientific, Singapore, 2001).

[54] E. Doedel, R. C. Paffenroth, A. R. Champneys, T. F. Fairgrieve, Y. A. Kuznetsov, B. E. Oldeman, B. Sandstede, and X. Wang, AUTO2000: Continuation and bifurcation software for ordinary differential equations (with HOMCONT), http://indy.cs.concordia.ca/auto/

[55] R. A. Satnoianu, P. K. Maini, and M. Menzinger, Physica D **160**, 79 (2001).

[56] A. Yochelis, E. Knobloch, Y. Xie, Z. Qu, and A. Garfinkel, EPL **83**, 64005 (2008).

[57] J. Kosek, H. Ševčíková, and M. Marek, J. Phys. Chem. **99**, 6889 (1995).

[58] M. Kærn and M. Menzinger, Phys. Rev. E **65**, 046202 (2002).

[59] A. Yochelis and M. Sheintuch, Phys. Chem. Chem. Phys. **11**, 9210 (2009).

[60] F. Zhang, M. Mangold, and A. Kienle, Chem. Eng. Sci. **61**, 7161 (2006).

[61] D. A. Smith and R. M. Simmons, Biophys. J. **80**, 45 (2001).

[62] G. A. Truskey, F. Yuan, and D. F. Katz, *Transport Phenomena in Biological Systems* (Pearson Prentice-Hall, NJ, 2004).

[63] A. V. Kuznetsov and K. Hooman, Int. J. Heat Mass Transfer **51**, 5695 (2008).